Laser-Based Non-Destructive 3D Scanning of Marine Coatings

Petersen, Christian Rosenberg; Rajagopalan, Narayanan; Israelsen, Niels Møller; Hansen, Rasmus Eilkær; Markos, Christos; Weinell, Claus E.; Kiil, Søren; Bang, Ole

Publication date:
2022

Document Version
Publisher's PDF, also known as Version of record

LASER-BASED NON-DESTRUCTIVE 3D SCANNING OF MARINE COATINGS

Christian Rosenberg Petersen[1], Narayanan Rajagopalan[2], Niels Møller Israelsen[1], Rasmus Eilkær Hansen[1], Christos Markos[1], Claus E. Weinell[2], Søren Kiil[2], and Ole Bang[1].

ABSTRACT

Optical coherence tomography (OCT) is presented as a field-applicable, non-contact, and non-destructive imaging technique for performing sub-surface inspection of marine coatings. The method is based on broadband mid-infrared supercontinuum laser light to significantly increase the imaging depth and resolution. The OCT system was able to image sub-surface structures, such as cracks and defects, as well as detect substrate corrosion through 369 μm of highly scattering marine coating. The system was also put into the field to show its applicability in an industrial marine environment. OCT imaging therefore has the potential to provide information about the sub-surface coating and substrate environment on marine structures and vessels, which is difficult to achieve using traditional methods.

KEY WORDS

NDT; non-destructive; non-contact; coatings; corrosion; defect; inspection; maintenance; OCT; supercontinuum; laser;

INTRODUCTION

Non-destructive testing (NDT) is an important part of assuring the performance and lifetime of protective coatings both in development, production, and in the field. To assess the quality of a coating, it is important to measure the thickness and detect any internal defects or delamination from the substrate. One technique, which has so far been largely missed by the NDT community, is optical coherence tomography (OCT). OCT is a reflection modality method originally developed for medical imaging based on the interference of light reflected/scattered from different depths of a sample, and because it is based on low intensity laser light it can reach microscopic resolution, is non-destructive, and does not require a contact medium. The challenge of OCT is that light is gradually lost when propagating through a sample due to scattering and absorption, so the penetration depth is very limited. Compared to a more widespread NDT technology like high frequency ultrasound, OCT does not penetrate as far (usually less than 1 mm), and is very sensitive to the particle size. On the other hand, ultrasound cannot resolve any details of the first few hundred microns from the surface, so in that case OCT can be complementary to existing ultrasound NDT.

One way to improve the penetration of OCT is to employ longer wavelengths of light, which results in reduced scattering. When moving towards longer wavelengths, physics unfortunately dictate that the spatial resolution is proportionally reduced. However, the depth resolution in OCT depends not only on the wavelength of light, but also the bandwidth of the light source (i.e. the span/spectrum of different wavelengths combined). Luckily, there is type of broadband laser that can extend far into the infrared: Supercontinuum (SC) lasers [1,2]. SC refers to the process whereby a relatively narrowband but high intensity laser pulse is gradually broadened in a nonlinear optical medium, such as an optical fiber. Using this technology, researchers have demonstrated various applications within spectroscopy and imaging, including OCT. There has been few reports of OCT being applied for inspection of coatings, primarily for cultural heritage preservation, but also for automotive and industrial coatings [3–10]. Marine coatings in particular make use of functional additives, which are highly scattering to visible and near-infrared light, and so there is a need for developing OCT systems based on longer wavelength mid-infrared light to improve the penetration depth. We recently demonstrated such a system for non-destructive, near real-time inspection of highly scattering samples, such as ceramics and polymers, as well as complex structures including the internal circuitry of a credit card chip [11]. In this paper we present the results of a recently finished project by the name SHIP-COAT (Sub-surface, High-resolution Inspection of Paints and Coatings using nOn-destructive lAser Tomography). In the project, OCT was evaluated as a NDT technique for inspecting marine coatings, including monitoring the curing process and detecting cracks and defects in

[1] DTU Fotonik, Department of Photonics Engineering, Technical University of Denmark, 2800 Kgs. Lyngby, Denmark.
[2] DTU Kemiteknik, Department of Chemical Engineering, Technical University of Denmark, 2800 Kgs. Lyngby, Denmark.

coatings exposed to extreme environments [12]. Towards the end, a transportable mid-infrared OCT system based on a robotic-arm was taken to a boat wharf in Copenhagen to demonstrate that the technology can be applied in the field.

METHODS

Optical Coherence Tomography

The MIR OCT system is based on a custom-built MIR supercontinuum (SC) laser, a free-space Michelson interferometer, and a specialized detection system that converts the mid-infrared light to near-infrared light, to allow for faster and more sensitive detectors to be used [13]. The mid-infrared SC laser is filtered such that the spectrum covers from 3.2-4.8 μm in wavelength, and about 20 mW of power is illuminating the sample. The broad spectrum of the SC laser results in an axial (depth) imaging resolution of about 6 μm, and the scanning lens used provides a lateral resolution of about 15 μm [14]. Images are created by scanning the laser-beam across a sample using galvanometric scanning mirrors with a variable integration time that allow for scanning with up to kHz line rates. A 3-5 mm scan with 1000 points takes between 0.3-3 seconds to capture depending on integration time. For more highly scattering coatings, a longer integration time is generally needed. The resulting 2D cross-section image is called a B-scan, and by also scanning the beam in the orthogonal direction a 3D volume or C-scan is made. A schematic of the system is shown in Figure 1.

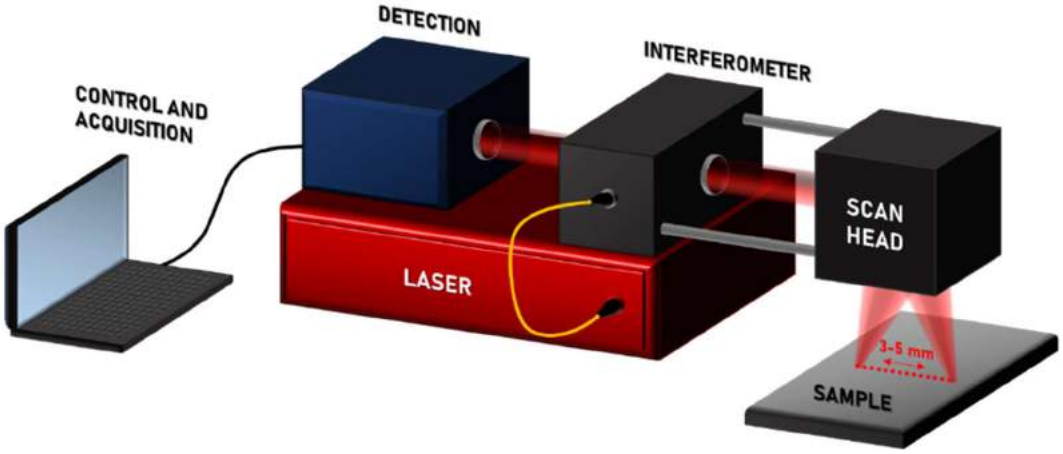

Figure 1. Schematic illustration of the MIR OCT system.

Sample preparation

High-pressure, high-temperature coating.
The coating was formulated using a DEN 438 epoxy novolac resin base with a functionality (f) of 3.6 and an m-xylylene diamine (MXDA) curing agent. The sample substrate was sandblasted carbon (mild) steel with dimensions 5 mm x 70 mm x 120 mm. Using a paintbrush of width 25 mm and aiming for a total dry film thickness (DFT) of 150 ± 25 μm, the coating was applied in two layers. The cured sample (Figure 2(a)) was subsequently immersed in salt water and exposed to a high pressure and high temperature (HPHT) environment, one of the extreme downhole application conditions of the oil and gas industry (for more information about the sample preparation and HPHT test see [15]). HPHT exposure of the coating led to three distinct zones with different degrees of coating degradation, as seen in Figure 2(b). In the region near the edge of the seawater level, a discrete red-colored deposition indicates the presence of iron oxide. From inspection of the sample using an optical microscope (Figure 2(c)), this region, in particular, had an abundance of cracks, and from preliminary inspection using OCT, this region showed the most subsurface features. Consequently, this zone was chosen for further inspection using OCT.

Commercial pigmented coatings.
Two commercial marine coatings were tested: (1) A blue-pigmented, self-polishing anti-fouling (AF) hull coating based on cuprous oxide (Cu2O) with a low self-polishing rate, and (2) a white-pigmented, high gloss (HG), alkyd enamel that is flexible and resistant to saltwater and other contaminants. The coatings were applied to line-polished aluminum substrates by a paintbrush and left to dry in a fumehood for min. 12 hours. For the corrosion detection measurements, a partially corroded aluminum substrate was used.

RESULTS

High-pressure, high-temperature coating

Figure 2(d) and 2(e) show a comparison between microscope images and OCT images of the coating surface near the iron oxide line. It is clear that OCT provides a significantly different contrast. The microscope images clearly show the iron oxide line and crystalline-like appearance of the salt water exposed region, whereas OCT highlights the finer surface structure and various defects, such as cracks and pits. Several cracks are clearly seen at points P1, P2, and P4, while the iron oxide line at P3 is barely distinguishable. Figure 2(f) show OCT B-scans revealing the subsurface structure of the coating. The top image shows a B-scan of an unexposed sample, revealing the high degree of roughness of the substrate compared to the relatively smooth surface. The only noticeable feature is a single point close to the surface indicated by a white arrow, which could be a small defect in the coating or simply part of the substrate. At P1 the presence of a crack can be seen from the feature appearing in the middle of the coating layer accompanied by a gap in the coating surface. The crack at P2 is seen more clearly because it runs parallel to the scan direction. At the iron oxide line P3 the only noticeable feature is a point of heightened substrate level accompanied by a small hole at the surface. Lastly, in P4 a group of three cracks meet and forms a complex structure below the surface, which is only partially captured by the B-scan. These images demonstrate how OCT can be used for monitoring the formation of subsurface cracks and defects due to exposure.

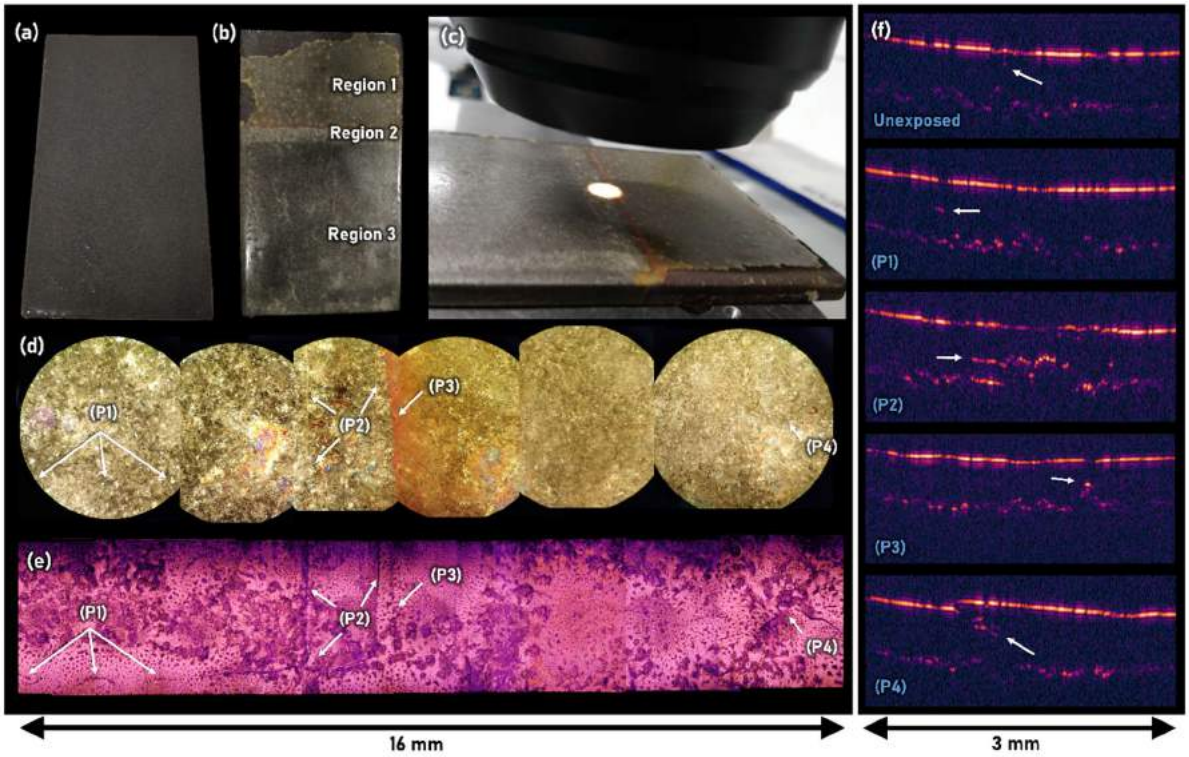

Figure 2. (a) Photograph of the coated steel sample. (b) Photograph of the coated sample after HPHT exposure. (c) Photograph showing the inspection region of the microscope. (d,e) Mosaic composite of microscope and OCT images, respectively, covering around a 3x16 mm area near the iron oxide line. (f) OCT cross-section images of unexposed and exposed samples near positions P1-P4.

Commercial coatings

Corrosion detection.

Figure 3 show a proof-of-concept demonstration of substrate corrosion detection using OCT. Figure 3(a) is a photo of the sample, where the commercial HG alkyd enamel was applied to a partially corroded aluminum plate. An OCT B-scan near the edge of the coated area is shown in Figure 3(b). Once cured, the coating was scribed with a scalpel at the interface between the corroded and non-corroded part of the plate, and a 3D scan was performed near the scratch. Figure 3(c) and 3(d) show a top-view projection of the scan at the coating surface, and at the coating-substrate interface, respectively. Corrosion is clearly

detected through the entire layer, which was estimated to be up to 369 µm thick [12]. Figure 3(e) is an ImageJ 3D visualization of the scan, applying a transparency of 40 and the GEM colormap. OCT therefore show promise as a method for early detection of corrosion onset at the coating-substrate interface.

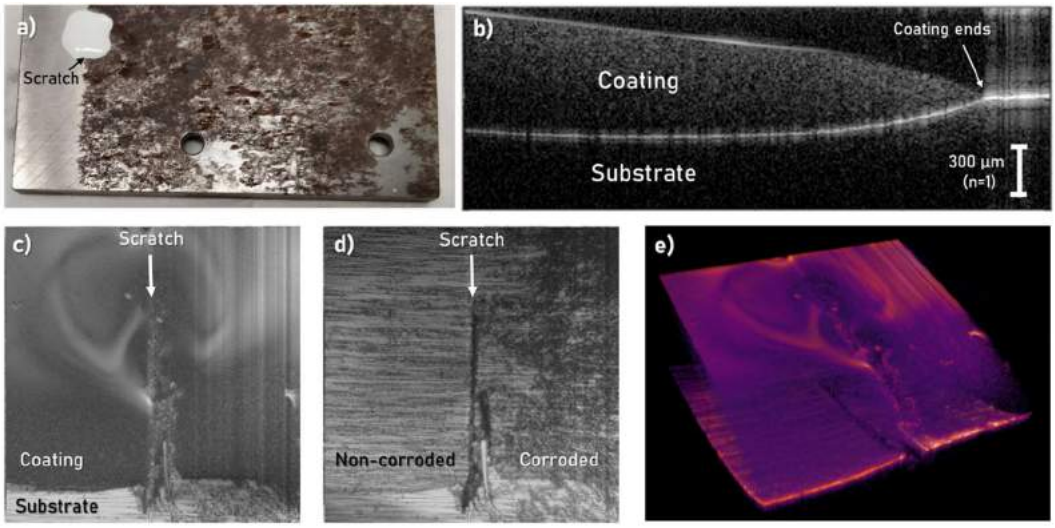

Figure 3. (a) Photograph of the HG coating applied to a partially corroded aluminum sample. (b) OCT B-scan near the edge of the coating. (c,d) Top-view projection of the scan at the coating surface, and coating-substrate interface, respectively. (e) ImageJ 3D visualization of the scan.

Detection of other defects.

Figure 4 shows a series of cases with OCT inspection of coatings. Figure 4(a) is a B-scan of the blue-pigmented AF coating containing Cu_2O particles, as seen in the microscope image of Fig. 4(b). Once cured, the surface of the coating is very rough, which combined with the many large Cu_2O-particles inhibits clear detection of the substrate. However, by averaging a number of adjacent scans it is possible to clearly see the coating-substrate interface to e.g. estimate the thickness or identify defects. Figure 4(c) show another case, where the HG coating is applied on top of a thinner layer of AF coating. In this case, OCT was able to detect a Cu_2O-particle that had diffused from the AF coating towards the surface. A similar case is shown in the microscope image of Fig. 4(d). Other interesting cases include detection of possible delamination (Fig. 4(e)), multiple HG-layer boundaries (Fig. 4(f)), and bubbles/voids (Fig. 4(g)).

Field operation.

As mentioned in the introduction, the OCT system was also tested under field conditions. To accommodate curved surfaces and larger reach, the galvanometric scanner was replaced with a robotic arm (Universal Robots UR5-e), and the interferometer was built into a probe that was mounted at the end of the arm, as shown in Figure 5(a). Operation of the system at a Copenhagen boat wharf is shown in Figure 5(b) and 5(c). The latter also show one of the issues encountered during testing, which is condensation and humidity. This is an issue because water absorbs light in the mid-infrared, reducing the depth from which a signal can be seen. Another issue is the poor coating surface quality of the tested hulls, as is evident from Figure 5(d). For instance, the hull showed signs of barnacles that had not been completely removed, and was thus visible through the coating. A B-scan of the coated barnacle surface is shown in Figure 5(e). B-scans from other parts of the hull also reveal multiple layers, and defects such as voids under the surface of the coating (see Figure 5(e,f)). This field test thus establishes that the technology can be brought out of the lab and into a marine environment to perform non-destructive inspection.

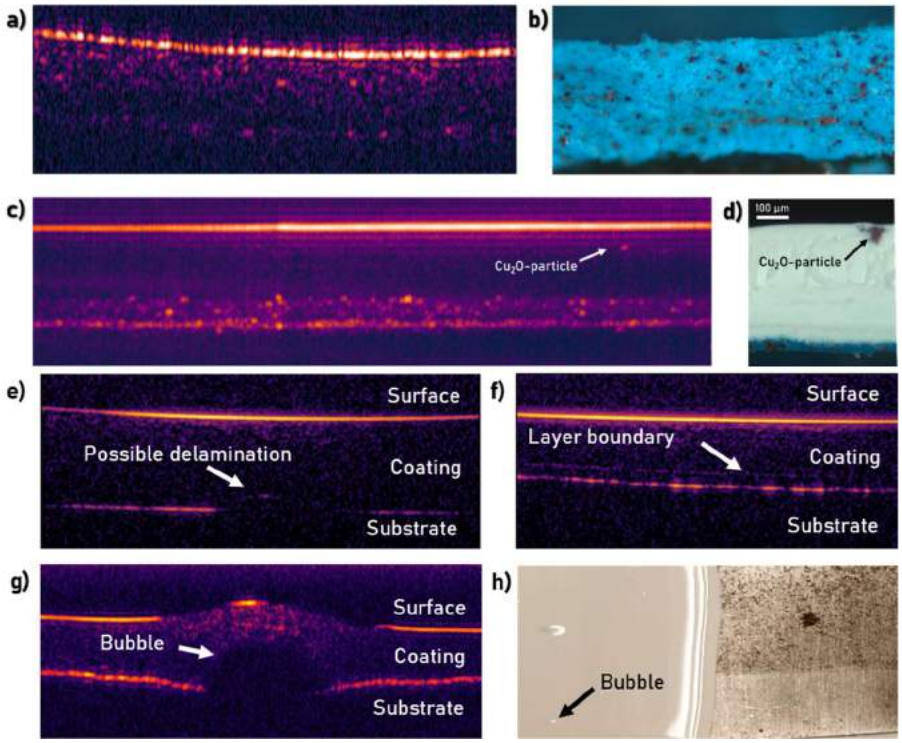

Figure 4. Various OCT images of structures, defects, and interfaces. (a,b) OCT B-scan and photograph of AF coating cross-section, respectively. (c,d) Detection of Cu_2O particle from the AF coating that has diffused into the HG coating. (e-f) OCT images of various defects in the HG coating. (h) Photograph of the HG coated sample, indicating the position of the bubble.

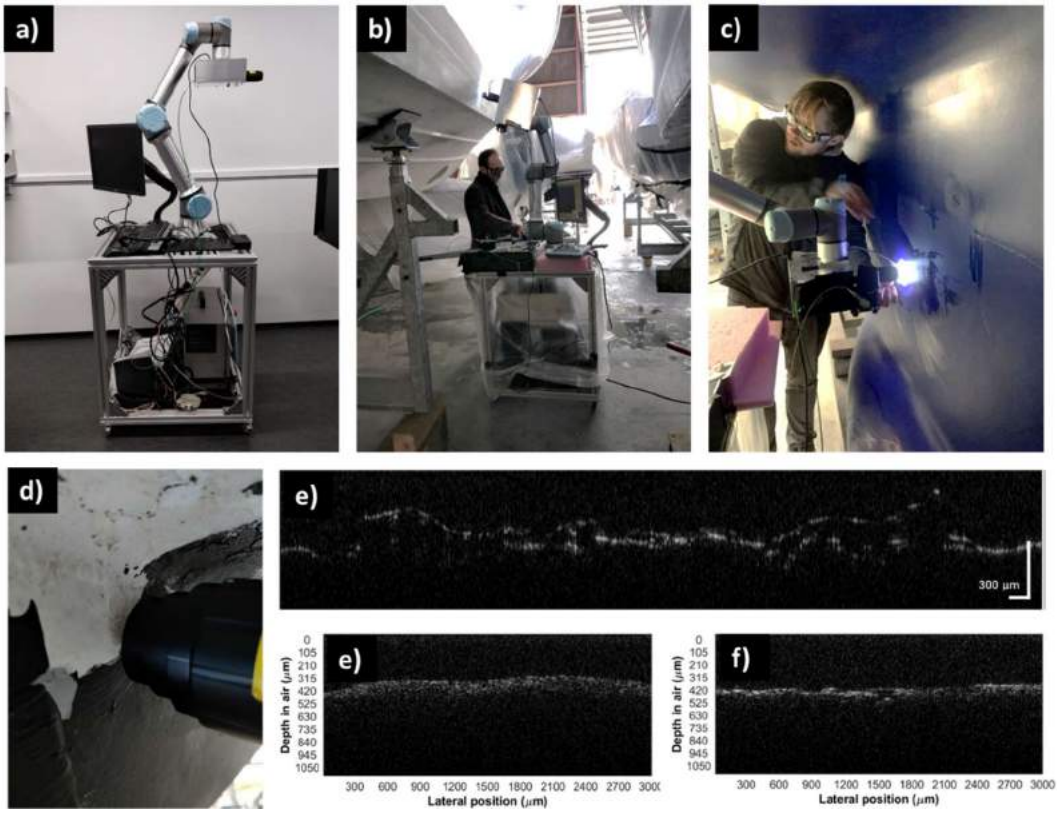

Figure 5. Field transportable OCT system. (a-c) Photographs of the system. (d) Photograph of a coated hull that showed signs of barnacle growth. (e-f) B-scans from the hull acquired using the field system.

CONCLUSIONS

In this paper, it was demonstrated how OCT based on mid-infrared supercontinuum light can be used for subsurface inspection of coatings. The technique was shown to be useful for imaging cracks and defects below the surface, including detection of substrate corrosion through 369 µm of HG coating. The penetration depth of OCT was found to be highly dependent on the surface roughness and particle size, limiting the useful imaging depth in highly scattering coatings, such as AF coating, to just a few hundred microns. The system was also tested at a boat wharf under field conditions, which revealed an issue with scanning in high humidity and condensation, as well as dirty and rough hull surfaces. With further development of the technology, OCT is believed to have great potential as a non-destructive imaging technique for industrial inspection of marine structures and vessels.

ACKNOWLEDGEMENTS

The authors acknowledge financial support by The Danish Maritime Fund in the project “SHIP-COAT” (project no. 2019-137).

REFERENCES

1. C. R. Petersen, U. Møller, I. Kubat, B. Zhou, S. Dupont, J. Ramsay, T. Benson, S. Sujecki, N. Abdel-Moneim, Z. Tang, D. Furniss, A. Seddon, and O. Bang, "Mid-infrared supercontinuum covering the 1.4–13.3 µm molecular fingerprint region using ultra-high NA chalcogenide step-index fibre," Nat. Photonics **8**(11), 830–834 (2014).
2. J. M. Dudley, G. Genty, and S. Coen, "Supercontinuum generation in photonic crystal fiber," Rev. Mod. Phys. **78**(4), 1135–1184 (2006).
3. C. S. Cheung, J. M. O. Daniel, M. Tokurakawa, W. A. Clarkson, and H. Liang, "Optical coherence tomography in the 2-µm wavelength regime for paint and other high opacity materials," Opt. Lett. **39**(22), 6509–6511 (2014).
4. M. Lenz, C. Mazzon, C. Dillmann, N. Gerhardt, H. Welp, M. Prange, and M. Hofmann, "Spectral Domain Optical Coherence Tomography for Non-Destructive Testing of Protection Coatings on Metal Substrates," Appl. Sci. **7**(4), 364 (2017).
5. P. Targowski and M. Iwanicka, "Optical Coherence Tomography: its role in the non-invasive structural examination and conservation of cultural heritage objects—a review," Appl. Phys. A **106**(2), 265–277 (2012).
6. Y. Dong, S. Lawman, Y. Zheng, D. Williams, J. Zhang, and Y.-C. Shen, "Nondestructive analysis of automotive paints with spectral domain optical coherence tomography," Appl. Opt. **55**(13), 3695–3700 (2016).
7. C. Wang, N. Zhang, Z. Sun, Z. Li, Z. Li, and X. Xu, "Recovering hidden sub-layers of repainted automotive paint by 3D optical coherence tomography," Aust. J. Forensic Sci. **51**(3), 331–339 (2019).
8. N. Zhang, C. Wang, Z. Sun, H. Mei, W. Huang, L. Xu, L. Xie, J. Guo, Y. Yan, Z. Li, X. Xu, P. Xue, and N. Liu, "Characterization of automotive paint by optical coherence tomography," Forensic Sci. Int. **266**, 239–244 (2016).
9. J. Zhang, B. M. Williams, S. Lawman, D. Atkinson, Z. Zhang, Y. Shen, and Y. Zheng, "Non-destructive analysis of flake properties in automotive paints with full-field optical coherence tomography and 3D segmentation," Opt. Express **25**(16), 18614–18626 (2017).
10. I. Zorin, P. Gattinger, M. Brandstetter, and B. Heise, "Dual-band infrared optical coherence tomography using a single supercontinuum source," Opt. Express **28**(6), 7858–7874 (2020).
11. N. M. Israelsen, C. R. Petersen, A. Barh, D. Jain, M. Jensen, G. Hannesschläger, P. Tidemand-Lichtenberg, C. Pedersen, A. Podoleanu, and O. Bang, "Real-time high-resolution mid-infrared optical coherence tomography," Light Sci. Appl. 8:11 (2019).
12. C. R. Petersen, N. Rajagopalan, C. Markos, N. M. Israelsen, P. J. Rodrigo, G. Woyessa, P. Tidemand-Lichtenberg, C. Pedersen, C. E. Weinell, S. Kiil, and O. Bang, "Non-Destructive Subsurface Inspection of Marine and Protective Coatings Using Near- and Mid-Infrared Optical Coherence Tomography," Coatings **11**(8), 877 (2021).
13. A. Barh, P. J. Rodrigo, L. Meng, C. Pedersen, and P. Tidemand-Lichtenberg, "Parametric upconversion imaging and its applications," Adv. Opt. Photonics **11**(4), 952–1018 (2019).
14. N. M. Israelsen, P. J. Rodrigo, C. R. Petersen, G. Woyessa, R. E. Hansen, P. Tidemand-Lichtenberg, C. Pedersen, and O. Bang, "High-resolution mid-infrared optical coherence tomography with kHz line rate," Opt. Lett. **46**(18), 4558–4561 (2021).
15. N. Rajagopalan, C. E. Weinell, K. Dam-Johansen, and S. Kiil, "Degradation mechanisms of amine-cured epoxy novolac and bisphenol F resins under conditions of high pressures and high temperatures," Prog. Org. Coat. **156**, 106268 (2021).